Energy 257 (2022) 124713

Contents lists available at ScienceDirect

Energy

journal homepage: www.elsevier.com/locate/energy

Part-load efficiency boost in offshore organic Rankine cycles with a cooling water flow rate control strategy

Mohammad Ali Motamed*, Lars O. Nord

Department of Energy and Process Engineering, Norwegian University of Science and Technology—NTNU, Trondheim, Norway

ARTICLE INFO

Article history:
Received 28 February 2022
Received in revised form
7 June 2022
Accepted 30 June 2022
Available online 7 July 2022

Keywords:
Control strategy
Process modeling and simulation
Equipment footprint
Offshore heat and power
Sliding pressure
Variable area nozzle turbine

ABSTRACT

Global concerns regarding greenhouse gas emissions and global warming have necessitated the speed up in using renewable energies and more efficient use of fossil fuels in the oil and gas industry. Harvesting gas turbine heat by organic Rankine bottoming cycles has raised as a potential solution to cut carbon dioxide emissions in offshore oil and gas installations. Offshore power cycles are expected to operate most of their operational life at part-loads where they suffer from poor efficiency. The purpose of this article is to boost the part-load efficiency of offshore organic Rankine cycles and keep it as close as possible to the design value. Here an operational strategy based on cooling water flow control is developed and added to a sliding pressure control logic and a variable area nozzle turbine control strategy. An in-house tool is developed for the design of organic Rankine cycles and the simulation of off-design control strategies. A design methodology is presented to optimize the cycle power output while minimizing the cycle footprint offshore. The proposed control strategy was successful in keeping the part-load efficiency close to design value and achieving a 5% reduction of annual carbon dioxide emissions.

1. Introduction

Norway has decided to reduce the greenhouse gas (GHG) emissions by 40% in 2030 compared to the 1990 emission level and to become a low emission society by 2050 [1]. This will be part of a common effort to decrease the global warming effects on the planet. Offshore oil and gas installation will play a key role in reaching these goals. Almost a quarter of Norway's total emission comes from the Norwegian continental shelf (NCS) [2]. The petroleum industry is a sector that pays the highest price for carbon dioxide (CO_2) emissions in Norway. It has been estimated that companies operating in NCS have paid a total emission cost of 700–800 NOK per ton of CO_2 in 2020 [3].

Boosting the lifetime efficiency of gas turbine-based power generation systems has raised as a potential solution for offshore emission reduction. A more efficient power cycle requires less fuel per MWh power generated. With less fuel burnt, less CO_2 is released to atmosphere in the power generation process. The impact is noticeable as assessments show that 85% of CO_2 emission comes from gas turbines on the NCS [2]. The solution not only reduce emissions but also will address the concerns regarding high fuel prices in future energy scenarios. It can be expected that hydrogen as an energy carrier will have a 4–9 USD/kgH_2 total cost for production, transport, and transformation in 2030 [4].

Gas turbine waste heat can be recovered and used in a bottoming cycle to reduce emitted CO_2 per MWh in offshore platforms. The use of organic Rankine cycles (ORC) in offshore installations have some advantages over other types of bottoming cycles such as supercritical CO_2, air, and steam bottoming cycles. They are lighter, more compact, and can run autonomously with less man-hour required [5,6]. Growth in the use of renewable energies and varying power demand put gas turbines and the bottoming cycles in part-load operation as they will be used as backup energy supplies. ORCs will suffer a poor thermal efficiency at part-load since less heat is available from the gas turbine at part-load. It was shown in Ref. [7] that ORC thermal efficiency can drop to 65% of full load efficiency at 30% gas turbine load.

Some control strategies have been developed and proposed in the open literature to overcome the low part-load efficiency challenge and to handle the varying load conditions. A sliding pressure control strategy is suggested in Ref. [8], in which evaporation pressure is decreased at part-loads. Employing a partial admission

* Corresponding author.
E-mail address: mohammad.a.motamed@ntnu.no (M.A. Motamed).

https://doi.org/10.1016/j.energy.2022.124713

Nomenclature

A	heat exchanger effective area (m^2)
C	heat capacity (J/K)
CR	heat exchanger heat capacity ratio
c_f	skin friction factor
D	diameter (m)
e	Heat exchanger effectiveness
f	Fanning friction factor
h	enthalpy (J/kg)
k	thermal conductivity (W/mK)
$\dot{m}$	mass flow rate (kg/s)
N	rotational speed (rad/s)
Nu	Nusselt number
P	pressure (Pa)
Pr	Prandtl number
Q	heat energy
Re	Reynolds number
T	temperature (K)
U	overall heat transfer coefficient (W/m^2K)
$\dot{V}$	volume flow rate
Ns	turbine specific speed
$\dot{W}$	power (W)

Greek letters

α	convective heat transfer coefficient
η	efficiency
ρ	density (kg/m^3)
ε	surface roughness (μm)

Subscripts

amb	ambient conditions
cc	combined cycle
cold	heat exchanger cold side, or corrected
D	based on diameter
dp	design point
E	gas turbine exhaust
f	gas turbine fuel
GT	gas turbine
hot	heat exchanger hot side
in	inlet
max	maximum
min	minimum
net	total net power
ORC	organic Rankine cycle
out	outlet
PD	pump discharge
pump	related to pump
s	isentropic
SD	superheater discharge
turbine	related to turbine

turbine is proposed in Ref. [9] to reduce the turbine and the ORC capacity according to the amount of heat available to the cycle. The concept of off-design control using a variable area nozzle (VAN) turbine is suggested in Ref. [10]. The ORC part-load control strategy based on VAN turbine is then further developed and optimized in Ref. [11] for offshore applications with gas turbines waste heat as the heat source. A part-load operational strategy is introduced in Ref. [12] where some ORC power capacity is left unused at full load to facilitate a constant efficiency operation at part-loads. A comprehensive comparison carried out in Ref. [11] showed that the VAN turbine control strategy can outperform available control strategies and provide higher efficiency.

Two knowledge gaps are identified in the research about the efficient operation of offshore ORCs at part-load. The first one is that available part-load operational strategies cannot be merged for a further efficiency boost. Therefore, the part-load efficiency improvement is limited to a certain value in each control strategy. In this paper, a control strategy is proposed that not only can improve the part-load efficiency by itself, but also can be added to other existing operational strategies for a further efficiency boost at part-loads. The improvement is made possible by using a variable speed cooling pump that adjusts the cooling capacity in the heat rejection process. The second knowledge gap is that few works can be found in the open literature in which size, weight, and footprint requirements are considered in the development of off-design operational strategy of offshore ORCs. Heat exchangers have the highest share of capital cost and footprint in an offshore ORC system. In this work, the ORC is designed taking footprint into account as a key performance indicator.

This paper proposes an optimal design methodology for offshore ORCs and a part-load operational strategy based on the variable cooling capacity. An ORC cycle is designed according to offshore heat and power requirements. Afterward, a control strategy is proposed to boost the part-load efficiency. The suggested control logic is applied to two cases: a sliding pressure control logic and a VAN turbine control logic. The improvement made by the suggested control strategy is evaluated and highlighted quantitatively. This work's novelty lies in suggesting a new control strategy that not only can boost the ORC part-load efficiency but also can be added to other ORC control logics for further improvement of the efficiency. The proposed logic can be implemented in a retrofit process and is considered as a low-hanging fruit to achieve. CO_2 emission will be reduced as the cycle thermal efficiency is increased in the presented work.

2. Method

The following method was developed to achieve the objectives defined in the scope of this work. The combined cycle configuration is selected for a gas turbine as the topping cycle, an intermittent heat transfer unit, an ORC cycle as the bottoming cycle, and a water-cooled heat rejection unit (Fig. 1). A baseline cycle is designed through a parametric study based on key parameters and performance indicators. The baseline control logic considered here is a sliding pressure strategy that regulates the ORC pump speed to control the cycle pressures and temperatures. The control logic for the heat rejection process is developed and added to two cases: 1) the baseline control strategy and 2) the VAN turbine part-load control strategy.

2.1. System configuration and layout

The process heat extraction and the ORC bottoming cycle are placed in a cascade layout. The reason is that in a cascade configuration, changing the process heat demand does not affect the produced power by the ORC with a constant heat source

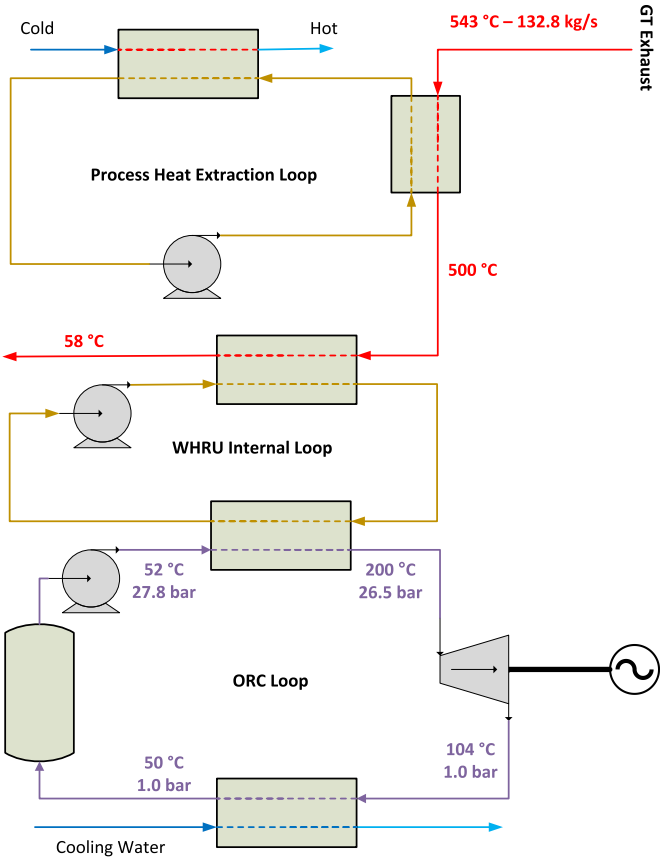

Fig. 1. Combined cycle configuration.

temperature [13]. The main source of power is a Siemens SGT-800 gas turbine providing 47 MW power at ISO conditions [14]. SGT-800 as a single shaft gas turbine has the advantage of being able to operate eighter with constant exhaust temperature or with constant exhaust mass flow rate for optimal load control in offshore combined cycles. The variable guide vanes in the gas turbine compressor make it possible to reduce the mass flow rate to 60–70% of the design flow rate and deliver the exhaust gas at a constant temperature to the bottoming cycle at reduced loads [15].

Process heat is extracted before the ORC cycle to guarantee the availability of the heat required for the platform installations. This is a key feature considering the use of wind energy for part of the electric power requirements of the offshore installation. All heat to the installation is provided by the process heat extraction loop and its availability vital. Natural organic fluids, in this case hydrocarbons, have the drawback of relatively low autoignition temperature [16]. Therefore, direct contact of the organic fluid and the hot exhaust gas is prevented by employing an intermittent oil loop heat transfer unit in the heat recovery section. As small leakages are inevitable in the heat exchanger, safety precautions have been considered by introducing the intermittent loop. Although this would increase the capital cost and the footprint of the system by adding an extra heat exchanger, safety has a higher priority in oil and gas installations. The other advantage of using an intermittent heat transfer unit is to prevent the thermal decomposition of the organic fluid components. Oil loop mass flow rate can be adjusted to provide heat to the cycle with a favorable low temperature. The evaporator temperature difference is then designed to reduce the chance of having hot spots in the organic fluid passing through the evaporator or the superheater.

The turbine used to extract power in the bottoming cycle is a fixed geometry expander in the sliding pressure control logic and a variable geometry turbine in the VAN turbine control strategy. A VAN turbine uses pivoted stator blades to adjust the turbine capacity without considerable change in the pressure or temperature of the turbine [17]. The ORC pump and cooling water pump are variable frequency drive (VFD) pump types to facilitate cycle control and cooling process control by manipulating the pumps speed. The condensing media is seawater and is assumed to be supplied at 15 °C or lower.

2.2. Component performance model

The component modeling approach is mainly based on the suggested methodology presented in Ref. [11]. Generalized process models are selected in the preliminary design stage where few detailed geometrical data are available from the system. Gas turbine performance data are the main boundary conditions forced to the ORC through the heat delivered to the bottoming cycle. GT MASTER 29 [18] is used to determine mass flow rate and enthalpy of gas turbine waste heat in load demands from 30% to 100% of full load condition. Gas turbine performance data are calculated in steady-state standard sea-level conditions, i.e., an ambient air temperature of 15 °C and an ambient pressure of 1.013 bar. Gas turbine efficiency is calculated based on the lower heating value (LHV) basis. A firing temperate control strategy is chosen for the gas turbine as it presented higher part-load efficiency than a constant exhaust temperature control logic. The off-design performance of the SGT-800 gas turbine is showed in Fig. 2.

A multi-stage variable speed centrifugal pump is selected for pressurizing the organic fluid in the cycle. A generalized performance prediction method for centrifugal pump in power plant applications is adapted from Ref. [8] and then is extended to a variable frequency drive pump case using the method suggested in Ref. [19]. Pump power consumption and discharge temperature is calculated through the following equations using the isentropic efficiency concept for the turbomachines.

$$\dot{W}_{pump} = \dot{m}_{pump} \frac{\Delta h_s}{\eta_{s,pump}} \tag{1}$$

$$T_{pump,out} = T_{pump,in} + \left(\frac{T_{pump,out,s} - T_{pump,in}}{\eta_{s,pump}} \right) \tag{2}$$

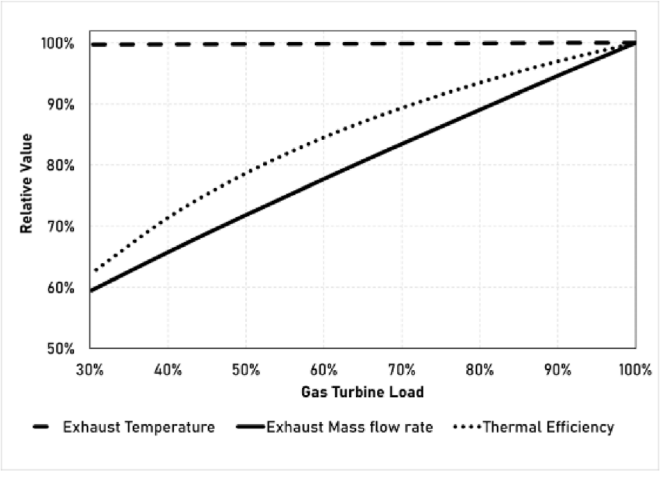

Fig. 2. SGT-800 gas turbine part-load performance.

Here $\dot{W}_{pump}$ is power consumed by the pump, $\dot{m}_{pump}$ is mass flow rate through the pump, Δh_s is the isentropic head rise by the pump and $\eta_{s,pump}$ is the isentropic efficiency of the centrifugal pump. T is fluid temperature, subscript s denotes isentropic conditions, *in* and *out* subscripts denote for inlet and outlet respectively. The pump mass flow rate and the enthalpy rise in varied speed conditions are calculated as presented in the following equations. Afterward, isentropic efficiency is estimated based on the model illustrated in Fig. 3.

$$\dot{m}_{pump} = \dot{m}_{pump,dp}\left(\frac{\rho}{\rho_{dp}}\right)\left(\frac{N}{N_{dp}}\right);\ \Delta h_{pump} = \Delta h_{pump,dp}\left(\frac{N}{N_{dp}}\right)^2 \tag{3}$$

In which, ρ is fluid density, $\dot{m}_{pump}$ is the mass flow rate, N is pump rotational speed, Δh denotes the head rise in the pump and *dp* denotes for design point conditions.

The radial inflow turbine performance is calculated based on the non-dimensional parameters presented in Ref. [20]. According to this methodology, the pressure ratio of a fixed geometry turbine is only a function of mass flow rate, inlet total thermodynamic conditions, and blade rotational speed. The functionality in the subsonic region is adapted from the work in Ref. [21] and illustrated in Fig. 4a for a generalized fixed geometry radial inflow turbine working at the design speed. The curve fitted to the model is as shown in the following equation and is used in the simulation tool. One should note that the correlation is valid only for the subsonic region of the turbine operation.

$$\frac{P_{turbine,\,out}}{P_{turbine,\,in}} = 5.493m_c^3 - 16.36m_c^2 + 16.40m_c - 4.531 \tag{4}$$

$$m_c = \left(\frac{\dot{m}}{\dot{m}_{dp}}\right)\left(\frac{T_{turbine,\,in}}{T_{turbine,\,in,dp}}\right)\left(\frac{P_{turbine,\,in}}{P_{turbine,\,in,dp}}\right)^{-1} \tag{5}$$

In which, $\dot{m}$ is turbine mass flow rate, m_c represents relative corrected mass flow rate, *dp* subscript denotes for design point conditions, *in* denotes for inlet location, P and T are total pressure and total temperature respectively. The design point is set in the subsonic region to allow for ORC load control in reduced gas turbine loads. However, this is achieved with a penalty in pressure ratio across the turbine. Although a supersonic turbine can provide higher power in the same flow capacity, the cycle flow rate can not be adjusted by manipulating the pressure ratio. Therefore, the design point is selected to be in the 5% margin of turbine choked region i.e., the design flow rate in the turbine is 95% of maximum turbine swallowing capacity which occurs at the coked turbine condition.

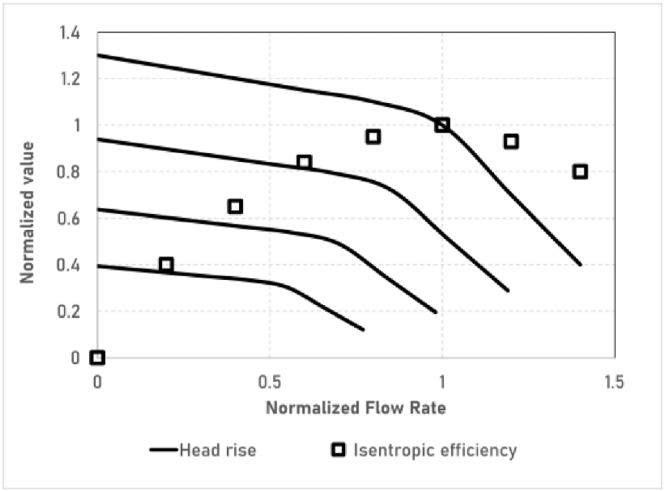

Fig. 3. ORC pump performance.

The model suggested in Ref. [22] is used for estimating the isentropic efficiency of the fixed geometry turbine. the model is based on the well-known turbine velocity ratio parameter and illustrated in Fig. 4b. Velocity ratio is defined as the ratio of turbine blade tip speed to the turbine isentropic speed and is well explained in Ref. [23]. The generalized curve is formulated based on enthalpy rise in the form of the following equation for easier use in the simulation tool.

$$\frac{\eta_{turbine}}{\eta_{turbine,dp}} = -2.570\left(\frac{\Delta h_s}{\Delta h_{s,dp}}\right)^{-1} + 3.326\left(\frac{\Delta h_s}{\Delta h_{s,dp}}\right)^{-1/2} - 0.084 \tag{6}$$

Here, $\eta_{turbine}$ is turbine isentropic efficiency, subscript *dp* denotes for design point condition, Δh is the turbine enthalpy rise, and subscript s represents the isentropic process.

The variable area nozzle turbine performance changes with the pivoted stators setting angel. An investigation in Ref. [21] showed that the capacity in a radial inflow turbine can be extended to a range of 20%–130% of design capacity by adjusting the variable nozzle vanes. However, the turbine suffers poor efficiency in capacities lower than 40% of design value. The turbine nozzle opening is calculated in each required set of pressure ratio and mass flow rate based on the model illustrated in Fig. 5a. Afterward, turbine specific speed is identified by the following equation. Knowing the turbine nozzle opening angle and the specific speed value, the turbine efficiency is calculated with the model presented in Ref. [21] (Fig. 5b).

$$Ns = \frac{N\dot{V}^{1/2}}{\Delta h_s^{3/4}} \tag{7}$$

Here, Ns represents the specific speed, N is turbine rotational speed, Δh is enthalpy rise across the turbine, Q is volumetric flow rate, and subscript s denotes the isentropic operation.

A generic model presented in Ref. [24] is used to estimate the size, heat transfer coefficient, and pressure loss in the heat exchangers. The heat absorption process is modeled as two series components: the economizer which accounts for the single-phase heat transfer, and an evaporator which accounts for the two-phase heat transfer. The evaporation and superheating are considered together in the evaporator section since a small degree of superheating (5 °C) is intended here. The generic model helps the designer to reach a realistic estimation of the performance, required heat transfer area, and volume of the heat exchangers when little detailed information is available in the early design stages. The following equations are used for the performance simulation of the condenser, evaporator, and economizer. It is assumed to have mean constant transport parameters for the flow inside the heat exchangers.

$$\frac{T_{hot,out} - T_{cold,in}}{T_{hot,in} - T_{cold,out}} = \exp\left[-\frac{UA}{C_{hot}}\left(1 - \frac{C_{hot}}{C_{cold}}\right)\right] \tag{8}$$

$$\dot{m}_{hot}\left(h_{hot,out} - h_{hot,in}\right) = \dot{m}_{cold}\left(h_{cold,in} - h_{cold,out}\right) \tag{9}$$

In which, subscripts *hot* and *cold* represent flow streams rejecting and absorbing heat respectively. T denotes for flow

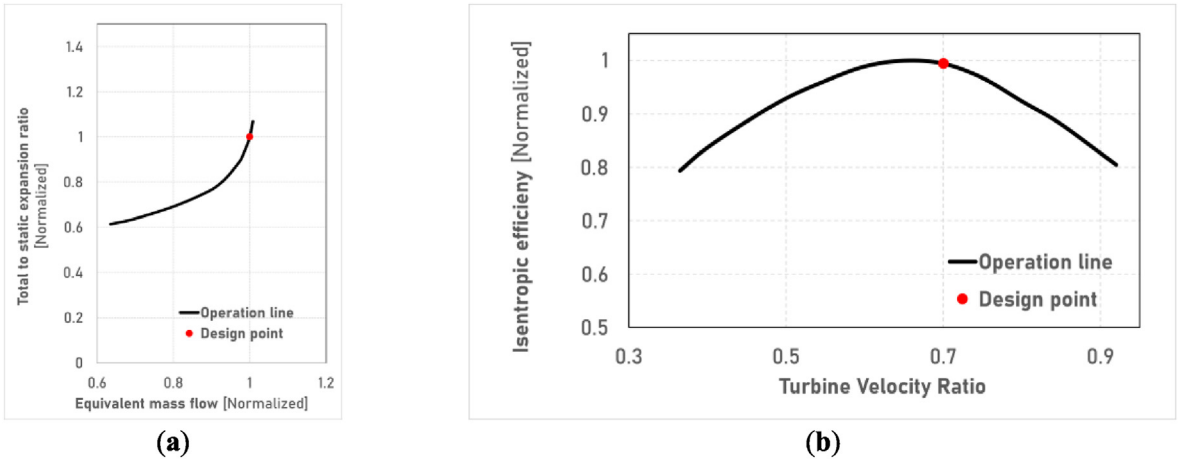

Fig. 4. Fixed-geometry turbine performance: (a) pressure ratio; (b) isentropic efficiency.

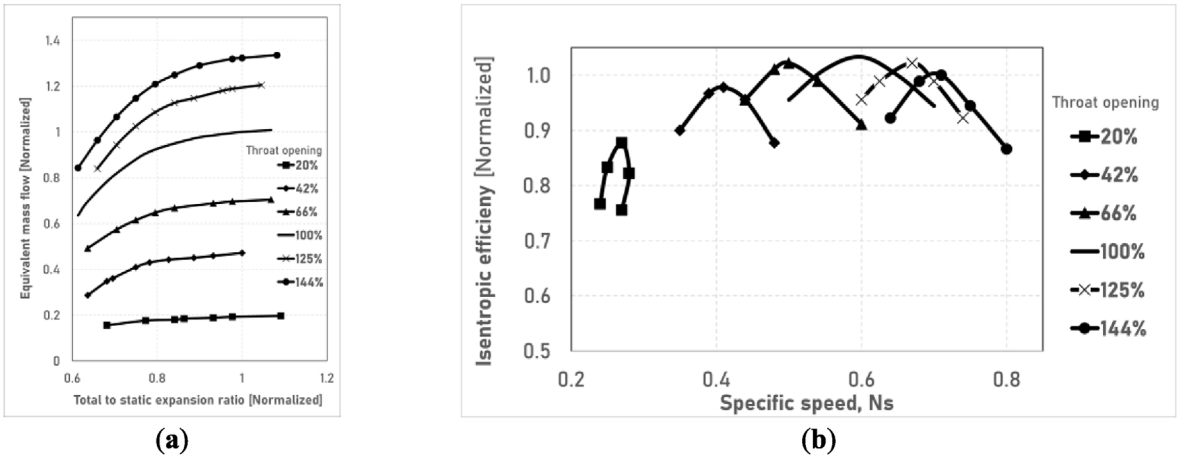

Fig. 5. Variable area nozzle turbine performance: (a) pressure ratio; (b) isentropic efficiency.

temperature, U is heat exchanger overall heat transfer coefficient, A is heat exchanger effective area, $\dot{m}$ is mass flow rate, h is the total enthalpy of the flow, C is heat capacity, *in* and *out* denote for inlet and outlet conditions, respectively. The heat exchanger effectiveness is defined as the ratio of actual heat transfer to the maximum amount of heat possible to be transferred. Heat exchanger overall heat transfer coefficient and the effectiveness can be related for a single-phase counterflow heat exchanger as in Ref. [25].

$$UA = \frac{C_{min}}{CR - 1} \ln\left[\frac{1 - \varepsilon}{1 - \varepsilon CR}\right] \tag{10}$$

$$CR = \frac{C_{min}}{C_{max}} \tag{11}$$

Here, CR is the heat capacity ratio of the fluids, U is heat exchanger overall heat transfer coefficient, A is heat exchanger effective area, C is flow heat capacity, ε is the heat exchanger effectiveness, *min* and *max* are lower and higher heat capacity of the flows inside the heat exchanger respectively. The fluid undergoes a phase change inside the evaporator. Therefore, it is not practicable to identify a unique single value for the heat capacity. It is suggested in Ref. [25] to set $C_{max} = \infty$ and consequently $CR = 0$ for analyzing the evaporator performance. Assuming equal effective heat transfer area for hot and cold flows, the overall heat transfer coefficient is formulated as a function of the convective heat transfer coefficient of each flow stream. The overall heat transfer coefficient is then expressed as the following equation based on the methodology presented in Ref. [26].

$$U = \left(\frac{1}{\alpha_{hot}} + \frac{1}{\alpha_{cold}}\right)^{-1} \tag{12}$$

$$\alpha = Nu\frac{k}{D} \tag{13}$$

In which, U is the overall heat transfer coefficient, α is convective heat transfer coefficient, Nu is the Nusselt number based on tube diameter, k is fluid conductivity and D is the average tube diameter in the heat exchanger. The effective area required in the heat exchangers to handle the heat load capacity is determined knowing the UA. Acceptable estimations for heat exchanger cross-sectional area, length and total volume are done assuming equal tube diameters and 100 μm surface roughness. The Nusselt number is estimated according to the methodology suggested in Ref. [24]. In this methodology, convective heat transfer coefficient correlates with friction factor in the pipe as is valid for the range of $2300 < Re < 5 \times 10^6$ and $0.5 < Pr < 2300$.

$$Nu = \frac{\left(Re_D - 10^3\right) Pr \frac{c_f}{2}}{1.0 + 12.7\sqrt{\frac{c_f}{2}}\left(Pr^{2/3} - 1\right)} \tag{14}$$

$$\frac{1}{\sqrt{f}} = -1.8\log_{10}\left[\left(\frac{\varepsilon/D}{3.7}\right)^{1.11} + \frac{6.9}{Re_D}\right] \tag{15}$$

Here, f is the fanning friction factor, c_f is friction factor in the heat exchanger pipe, ε/D is relative surface roughness, Re, Pr, Nu are the well-known parameters Reynolds number, Prandtl number and Nusselt number, respectively. The reference length in the nondimensional parameters is the tube diameter.

2.3. Cycle design

The bottoming cycle is usually designed for maximum power extraction from the gas turbine waste heat. However, increasing the power capacity of the cycle results in larger and heavier equipment. Larger heat exchangers and heavier turbines increase the footprint of the bottoming cycle in the offshore platform. Therefore, a compromise is made between the power output and the equipment size. A parametric study is conducted over the design decision parameters to optimize the key performance indicators while keeping the limitations in the allowable range. Combined cycle thermal efficiency is defined as the ratio of total net power to the energy supplied by fuel.

$$\eta_{cc} = \frac{\dot{W}_{net}}{Q_f} = \frac{\dot{W}_{GT} + \dot{W}_{ORC}}{Q_f} = \frac{\dot{W}_{GT}}{Q_f} + \frac{\dot{W}_{ORC}}{Q_f} = \eta_{GT} + \frac{\dot{W}_{ORC}}{Q_f} \tag{16}$$

Here η_{cc} is combined cycle efficiency, $\dot{W}_{net}$ is net shaft power delivered, Q_f is energy added by the fuel in the gas turbine, $\dot{W}_{GT}$ is gas turbine shaft power, $\dot{W}_{ORC}$ is shaft power delivered by the ORC, and η_{GT} is gas turbine thermal efficiency. Gas turbine exhaust heat (Q_E) can be related to the fuel heat energy using gas turbine thermal efficiency.

$$Q_f = \frac{Q_E}{1 - \eta_{GT}} \tag{17}$$

Gas turbine exhaust heat is calculated based on the available enthalpy in the exhaust flow stream.

$$Q_E = \dot{m}_{GT}(h_E - h_{amb}) \tag{18}$$

where $\dot{m}_{GT}$ is gas turbine exhaust mass flow rate, h_E is the enthalpy of exhaust flow at gas turbine discharge, and h_{amb} is the enthalpy of exhaust flow at the ambient conditions. Combining (16), (17), and (18) the formula for calculation of the combined cycle efficiency is reached.

$$\eta_{cc} = \eta_{GT} + \frac{(1 - \eta_{GT})\dot{W}_{ORC}}{\dot{m}_{GT}(h_E - h_{amb})} \tag{19}$$

equation (19) is used to estimate the combined cycle efficiency in this study. ORC thermal efficiency is defined as the ratio of the power generated by the ORC to the absorbed heat by ORC.

$$\eta_{ORC} = \frac{\dot{W}_{ORC}}{\dot{m}_{ORC}(h_{SD} - h_{PD})} \tag{21}$$

Here, $\dot{m}_{ORC}$ is the mass flow rate through ORC, h_{SD} is the enthalpy of the organic fluid at superheater discharge, and h_{PD} is the enthalpy of the organic fluid at the pump discharge. In a Rankine cycle with a known superheating degree, the thermodynamic cycle is fully established by determining the evaporation temperature and the condensing temperature. Design inputs and assumptions are tabulated in Table 1. ORC mass flow rate is designed to reach the minimum pinch point temperature difference (PPTD) allowed in the economizer cold side entrance. The minimum temperature difference in the cooling process happens inside the condenser where the organic fluid first enters the two-phase region. The cooling water flow rate is designed to hold the allowed PPTD in the condenser.

2.4. Part-load operation strategy

The ORC controller manipulates the tuning parameters to handle imposed operational conditions at part-loads. The varying operational conditions come from changes in gas turbine load demand which alter the mass flow rate and enthalpy of the waste heat available to the offshore bottoming cycle. Off-design values for the gas turbine exhaust heat are illustrated in Fig. 2. It was shown in Ref. [11] that for an offshore ORC with a fixed-geometry turbine, manipulating ORC pump speed and cooling pump speed is sufficient to establish a unique off-design operational point. ORC pump speed is tuned by the controller to adjust the evaporation pressure in the evaporator. Evaporation pressure is tuned at part-loads to achieve maximum power output from the ORC. This operational strategy is called a sliding pressure control strategy in which the evaporation pressure slides to optimize the cycle performance while handling the available heat to the cycle. Employing a variable geometry turbine adds a degree of freedom to the controller and allows for further improvement of the cycle efficiency at part-loads. The turbine blades opening angle is then adjusted to facilitate regulation of cycle mass flow rate almost independent of evaporation pressure.

The cooling water pump speed is responsible for controlling the condensation pressure in both sliding pressure and VAN turbine logic. In case of a gap between ORC condensation temperature and cooling water supply temperature, there is a potential to tune the cooling water flow rate to optimize the cycle power output in part-loads. In the proposed cooling flow control strategy, condensation pressure slides to allow for more efficient operation. The condensing pressure slides to allow for lower cycle pressures in the off-design conditions where less heat is available to the bottoming cycle. Fig. 6 illustrates ablatively how the thermodynamic cycle is controlled with a cooling flow control logic at part-load. The cooling flow control strategy is applied to both the sliding pressure and VAN turbine logic for a further efficiency boost.

The design and off-design methodology are implemented in an in-house design and simulation tool called ORCSIM. The tool is developed in the MATLAB framework to provide users with a fast and user-friendly design tool. The thermodynamic properties library is initiated by linking the CoolProp database to the in-house code. CoolProp is a comprehensive free thermodynamic database coupled to Python [27]. The tool is verified with data available in the open literature in both design and simulation modes [11]. It can do single-point design analysis, parametric study, off-design analysis, and optimization for a set of given part-load gas turbine performance characteristics.

3. Results and discussion

An ORC bottoming cycle is designed for an offshore gas turbine combined cycle to extract the highest possible work from the waste heat while minimizing the size and footprint. The off-design behavior of the designed cycle is investigated with two part-load

Table 1
Design inputs.

Gas Turbine		Bottoming Cycle	
power output [MW]	47.05	minimum heat exchanger PPTD [°C]	10
thermal efficiency [%]	37.48	pump isentropic efficiency [%]	70
exhaust gas mass flow rate [kg/s]	132.8	turbine isentropic efficiency [%]	80
exhaust gas temperature [°C]	452.7	condenser/economizer pressure loss [%]	5
process heat extraction [MW]	4.00	evaporator pressure loss [%]	1

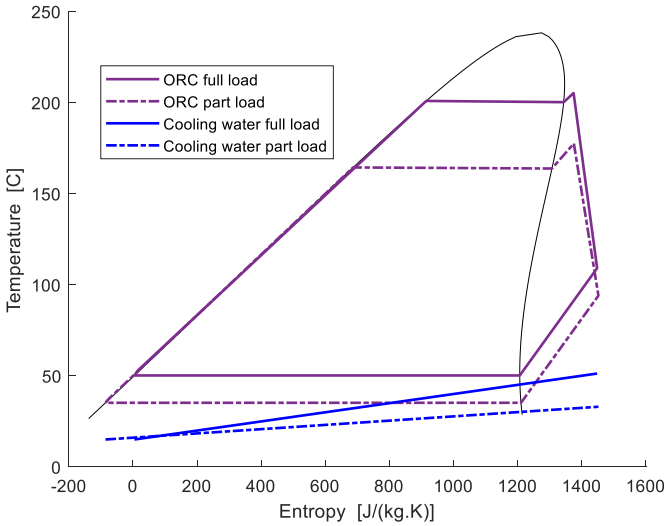

Fig. 6. Cycle thermodynamics at part-load with cooling flow control strategy.

operational strategies: sliding pressure and VAN turbine logic. Afterward, a control logic called the cooling flow control strategy is developed. The proposed strategy is added to the two baseline logics. The efficiency boost is investigated and illustrated to show the competency of the suggested solution.

3.1. Full-load design

Design assumptions and gas turbine full load performance data are tabulated in Table 1. The parametric study on the ORC performance is illustrated in Fig. 7. Key performance indicators are studied over the design choices (evaporation temperature and condensation temperature). Fig. 7a, b, and Fig. 7c show that higher ORC power output, ORC efficiency, and combined cycle efficiency occur in higher evaporation temperatures and lower condensation temperatures. However, this will be accompanied by a higher turbine pressure ratio which requires more stages in the turbines (Fig. 7d). Total effective area and total volume are defined for the heat exchangers used in the cycle to account for the footprint of the design. As shown in Fig. 7e and g, higher evaporation temperature and lower condensation temperature require more space to occupy and a larger effective area in the heat exchangers. The reason is that more heat is transferred to and from the cycle in the evaporator and condenser, respectively. To get a better insight into the pattern of ORC performance and footprint, a joint parameter is introduced to account for both. Specific total area and specific total volume represent the required footprint for each kW of ORC power in every design decision point. Fig. 7f and h show that lower specific area and volume in heat exchangers occur at higher evaporation and condensation temperatures. However, this cannot be the only basis for the design decisions since very low power capacity will happen at these points. The total volume of heat exchangers accounts for the required volume of condenser, evaporator, and economizer, overall. Fig. 8a, Fig. 8b and 8c illustrates what is the share of each of the heat exchangers in the total volume. It shows that evaporator volume can be neglected in comparison to the economizer and the condenser as most of the heat transfer takes place in the two latter.

The power output and footprint of the ORC compete each other in opposite directions. Therefore, a compromise is needed to establish the design decision. A total volume of 1160 m^3 is established as the maximum possible volume that can be occupied by the heat exchangers in the offshore installation. As shown in Fig. 8d, highest power output for a fixed heat exchanger volume happens in the highest possible condensing temperature. This can be explained by the fact that higher condensation temperatures need lower volume per kW due to higher fluid density in the heat exchangers and lower mass flow rate required in the ORC cycle (Fig. 8). With this reasoning, evaporation and condensation temperature are set for the design cycle (Table 2). With an established thermodynamic cycle and PPTD in the heat exchangers, ORC mass flow rate is determined. A five-degree superheating is assumed at the evaporator discharge to assure pure vapor entering the expander. Cyclopentane is chosen for the ORC working fluid with an auto-ignition temperature of 580 K [7]. In the working temperature conditions of the designed cycle, Cyclopentane has suitable pressure values while having less environmental impacts. Designed cycle specifications are tabulated in Table 2.

3.2. Part-load operational strategy

Improvements made by adding the proposed cooling flow control logic to the baseline sliding pressure operational strategy are illustrated in Fig. 9a. Calculations show that ORC efficiency at 30% gas turbine load falls to 85% of design value with the sliding pressure logic. However, it can be kept higher than 95% of design value in the range of 30%−100% of gas turbine load with the suggested cooling flow control logic. Two efficiency point improvement is observed in the combined cycle efficiency by applying the proposed cooling flow operational strategy at 30% gas turbine load (Fig. 9b). It is considered as a 5.2% relative reduction in CO_2 emission in an offshore combined cycle operating at 30%−50% load. It is shown in Fig. 10a that ORC part-load efficiency can be kept higher than 90% of design value with VAN turbine control logic, down to 30% gas turbine load. The presented cooling flow control logic further boosts the part-load ORC efficiency to 94% of design value at 30% gas turbine load. The combined cycle efficiency is improved for one point further by the suggested solution at a 30% gas turbine load (Fig. 10b). The outcome is a 2.6% further decrease in the CO_2 emission due to a boost in the part-load efficiency. The emission cut for 1% efficiency improvement of combined cycle efficiency is estimated to be 3-kiloton CO_2 yearly for a 47 MW gas turbine, assuming 250 g CO_2 emission per kWh.

A comparison is presented in Fig. 11 among sliding pressure logic, VAN turbine logic, and cooling flow control logic added to the baselines. It shows that ORC part-load efficiency can be improved to always stay higher than 94% of full-load efficiency with no major retrofit to the equipment. It can be achieved by replacing the fixed-speed cooling water pump with a VFD pump and upgrading the

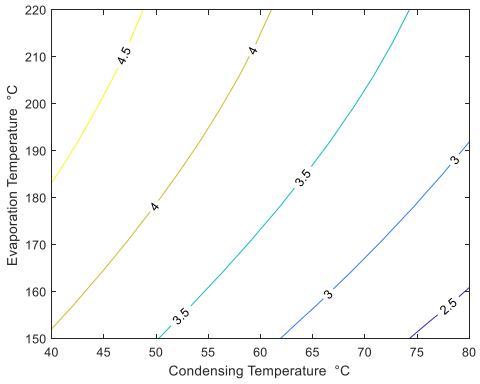

(**a**) ORC power [MW]

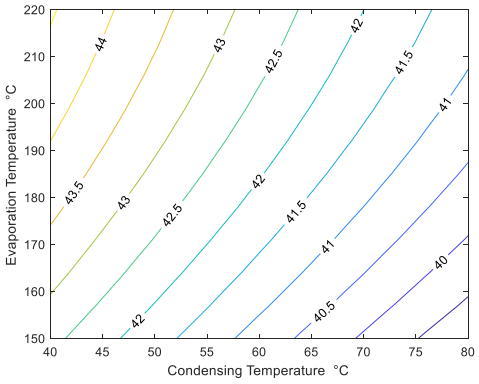

(**b**) η_{cc} [%]

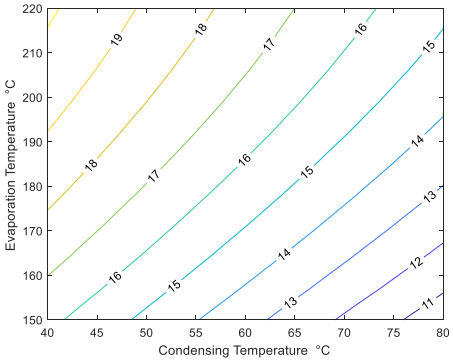

(**c**) η_{ORC} [%]

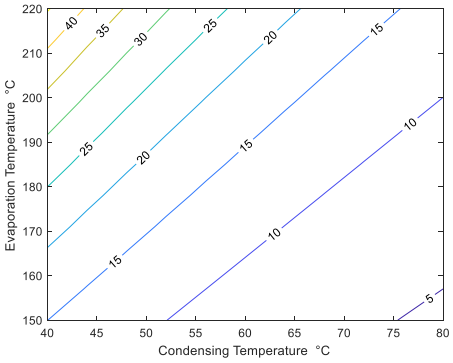

(**d**) ORC pressure ratio

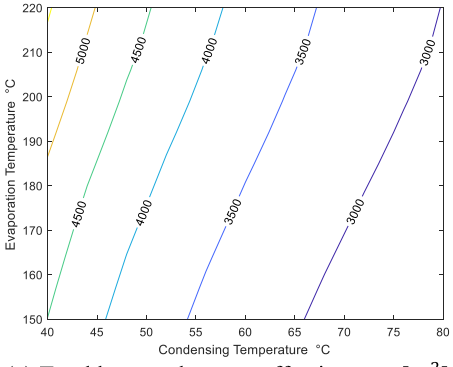

(**e**) Total heat exchangers effective area [m^2]

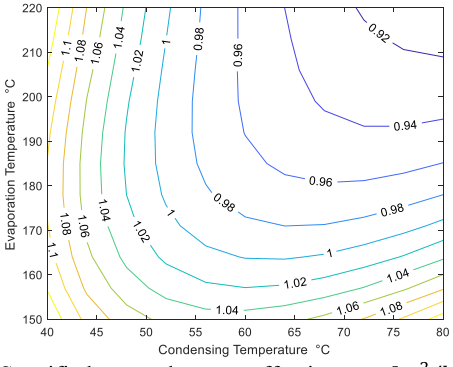

(**f**) Specific heat exchangers effective area [m^2/kW]

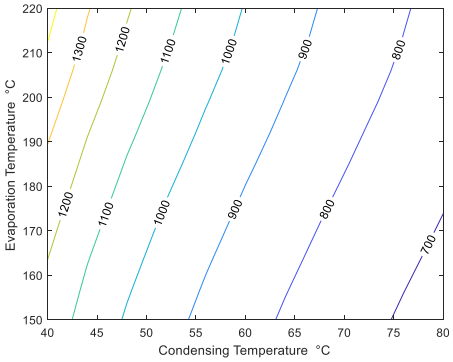

(**g**) Total heat exchangers volume [m^3]

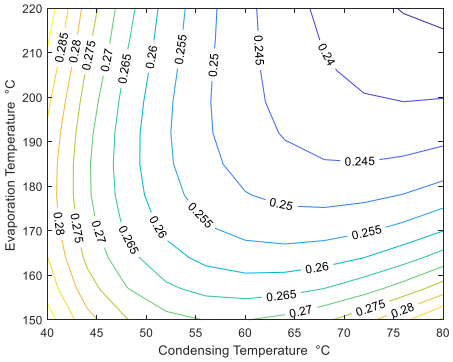

(**h**) Specific heat exchangers volume [m^3/kW]

Fig. 7. Design parametric study.

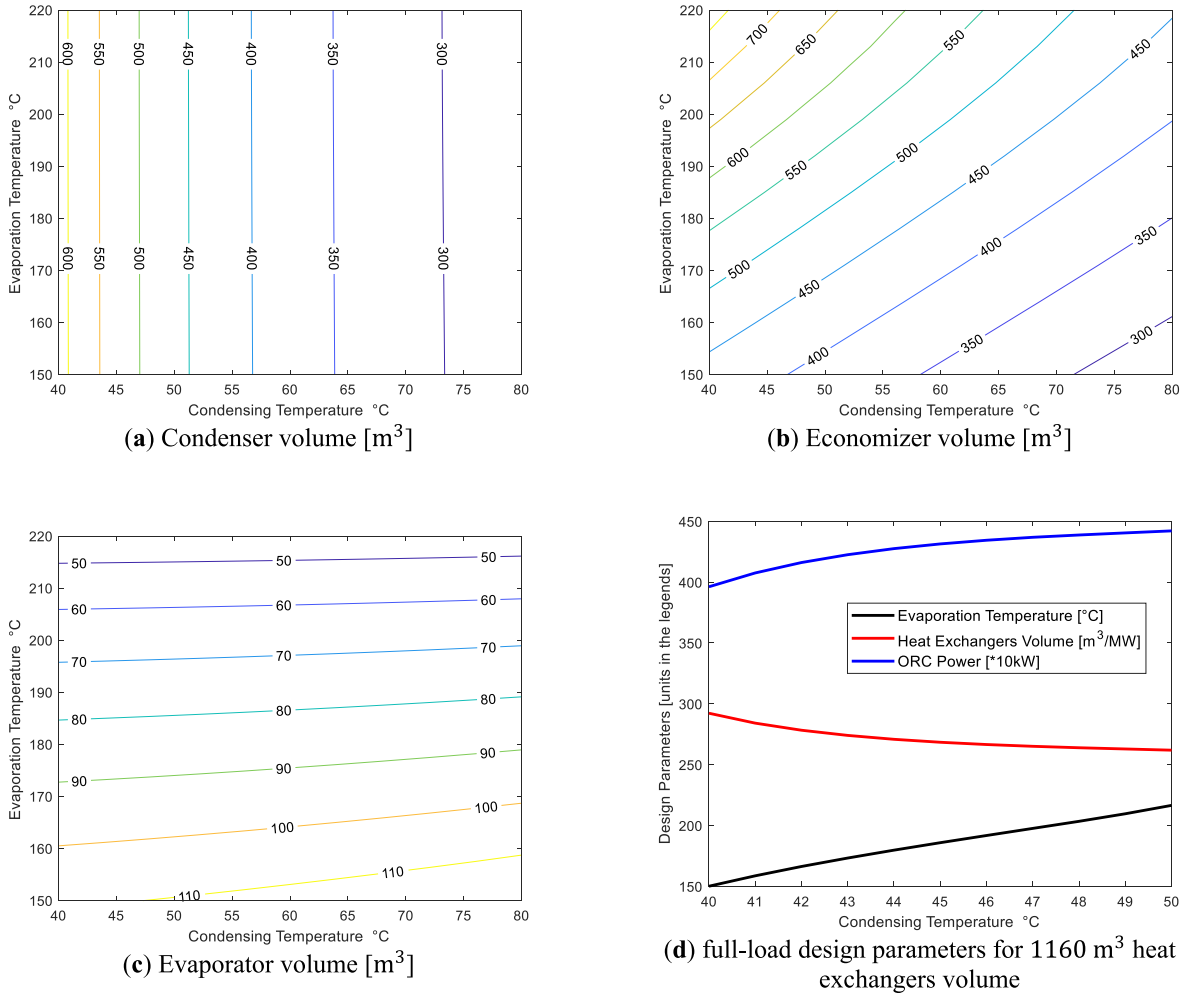

(**a**) Condenser volume [m^3] (**b**) Economizer volume [m^3]

(**c**) Evaporator volume [m^3] (**d**) full-load design parameters for 1160 m^3 heat exchangers volume

Fig. 8. ORC parametric study and design parameters.

Table 2
Designed ORC specifications.

Cycle properties	Value	Cycle properties	Value
evaporation temperature [°C]	200	power output [MW]	4.3
condensing temperature [°C]	50	combined-cycle efficiency [%]	43.3
turbine pressure ratio	24	mass flow rate [kg/s]	40.9
thermal efficiency [%]	18.1	air exhaust temperature [°C]	58
superheating [°C]	5	Heat exchanger PPTD [°C]	10

controller. The ORC efficiency is kept higher than 98% of full-load efficiency by adding employing a VAN turbine and a VFD cooling pump. The solution is compact and does not increase the footprint of the ORC in the offshore installation. Therefore, a VAN turbine with cooling flow control logic is suggested for the range of 60%–100% gas turbine loads, while sliding pressure with cooling flow control logic is a better solution for the 30–60% gas turbine loads. The advantage of the proposed solutions is that they can be merged

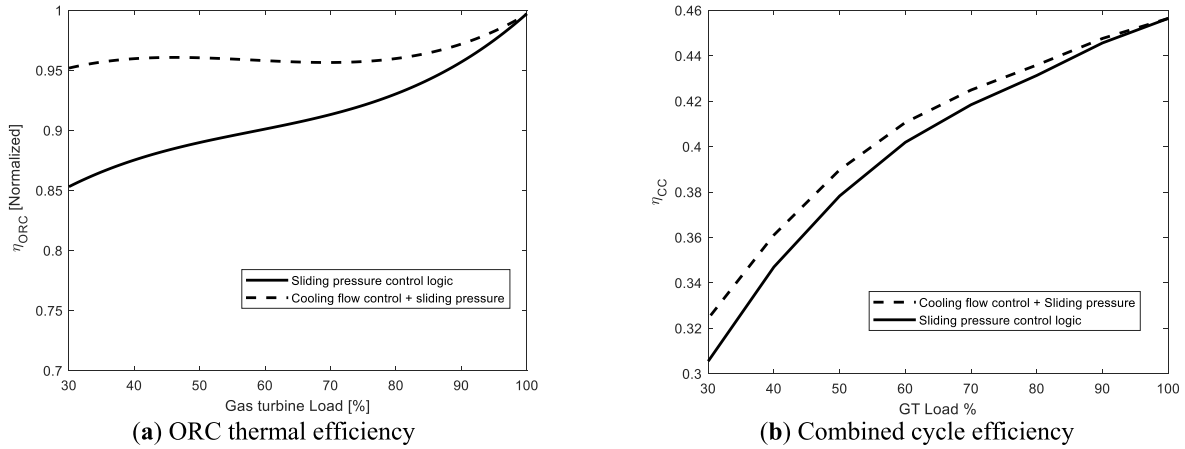

(**a**) ORC thermal efficiency (**b**) Combined cycle efficiency

Fig. 9. Part-load efficiency with sliding pressure and cooling flow control strategies.

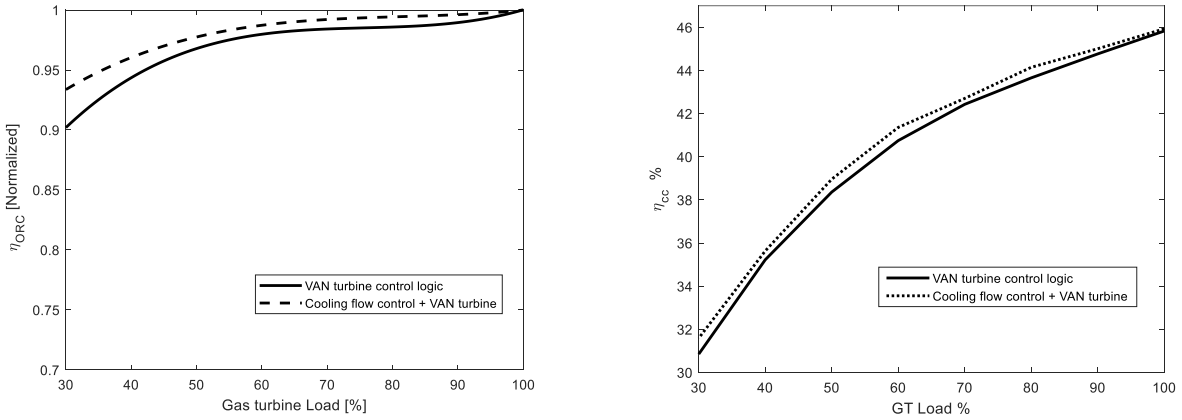

(**a**) ORC thermal efficiency (**b**) Combined cycle efficiency

Fig. 10. Part-load efficiency with VAN turbine and cooling flow control strategies.

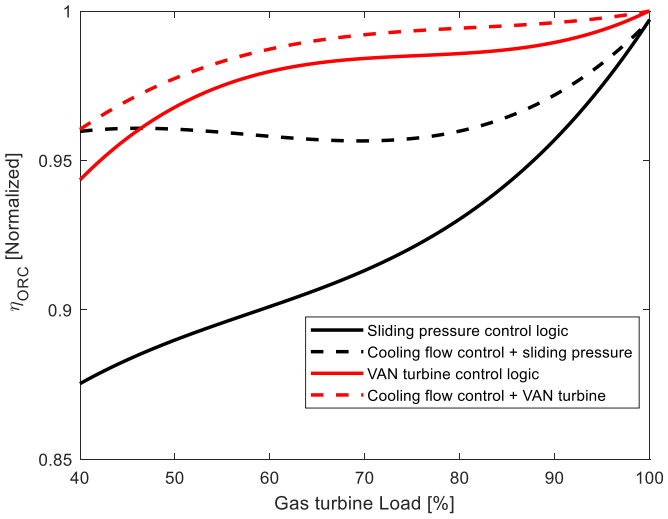

Fig. 11. Part-load efficiency of ORC with proposed control strategies.

and can be employed simultaneously in one system. Therefore, the operator can choose any combination of these three solutions.

4. Conclusion

An ORC bottoming cycle was designed to extract the maximum possible power from the gas turbine waste heat while minimizing the footprint of the cycle in the offshore platform. It was shown that a considerable temperature gap between supply cooling water and the ORC condenser allows for smaller footprint of the equipment in the specified volume available for the system. This potential was used to further boost the part-load efficiency by manipulating the cooling pump speed. Sliding pressure strategy with cooling flow control logic were suggested instead of VAN turbine with cooling flow control logic in 30%–60% gas turbine load range due to the same improvement with less complexity in the mechanism. However, VAN turbine with cooling flow control logic was suggested for the 60%–100% gas turbine load due to higher efficiency boost. The outcome of adding cooling flow control logic was a 10% further boost for the sliding pressure logic and a 5% further boost for the VAN turbine logic. A 5.2% reduction of CO_2 emission was estimated by employing the proposed solutions compared to the baseline control strategy. More detailed turbine performance investigation and study of the system dynamics are left for future works.

Author contributions

M.A.M. developed the modelling tool, carried out the simulations, formal data analysis, and wrote the manuscript. L.O.N. contributed to the critical analysis of the results, reviewed the manuscript, and supervised the work. Both share the effort of conceptualization of the idea. All authors have read and agreed to the published version of the manuscript.

Declaration of competing interest

The authors declare that they have no known competing financial interests or personal relationships that could have appeared to influence the work reported in this paper.

Data availability

Data will be made available on request.

Acknowledgement and Funding

This publication has been produced with support from the LowEmission Research Centre (www.lowemission.no), performed under the Norwegian research program PETROSENTER. The authors acknowledge the industry partners in LowEmission for their contributions and the Research Council of Norway (**296207**).

References

[1] Norwegian Ministry of Climate and Environment. Norway's national plan related to the decision of the EEA joint committee. 2019. 269.
[2] Budiono HR, Hakim C. Resource report; discoveries and fields. 2019.
[3] NPD. Exploration resource report 2020. 2020. p. 1–77 [Online]. Available: https://www.npd.no/en/facts/publications/reports2/resource-report/.
[4] IEA. The Future of Hydrogen: seizing today's opportunities. 2019. p. 203. Propos. Doc. Japanese Pres. G20, no. June.
[5] Bacci A, Asti A, Landi G, Scotti Del Greco A, del Turco P, Seghi G. THE ORegen TM WASTE HEAT RECOVERY CYCLE. REDUCING THE CO 2 FOOTPRINT BY; 2011. p. 1–10.
[6] Pierobon L, Benato A, Scolari E, Haglind F, Stoppato A. Waste heat recovery technologies for offshore platforms. Appl Energy 2014;136:228–41. https://doi.org/10.1016/j.apenergy.2014.08.109.
[7] Motamed MA, Nord LO. Improving the off-design efficiency of organic rankine. 2021. https://doi.org/10.14459/2021mp1632935.
[8] Hu D, Li S, Zheng Y, Wang J, Dai Y. Preliminary design and off-design

performance analysis of an Organic Rankine Cycle for geothermal sources. Energy Convers Manag 2015;96:175–87. https://doi.org/10.1016/j.enconman.2015.02.078.
[9] Casartelli D, Binotti M, Silva P, Macchi E, Roccaro E, Passera T. Power block off-design control strategies for indirect solar ORC cycles. Energy Proc 2015;69:1220–30. https://doi.org/10.1016/j.egypro.2015.03.166.
[10] Cao Y, Dai Y. Comparative analysis on off-design performance of a gas turbine and ORC combined cycle under different operation approaches. Energy Convers Manag 2017;135:84–100. https://doi.org/10.1016/j.enconman.2016.12.072.
[11] Motamed MA, Nord LO. Assessment of organic rankine cycle part-load performance turbine technology. Energies 2021;14(23). https://doi.org/10.3390/en14237916.
[12] Muñoz De Escalona JM, Sánchez D, Chacartegui R, Sánchez T. Part-load analysis of gas turbine & ORC combined cycles. Appl Therm Eng 2012;36(1):63–72. https://doi.org/10.1016/j.applthermaleng.2011.11.068.
[13] Nami H, Ertesvåg IS, Agromayor R, Riboldi L, Nord LO. Gas turbine exhaust gas heat recovery by organic Rankine cycles (ORC) for offshore combined heat and power applications - energy and exergy analysis. Energy 2018;165:1060–71. https://doi.org/10.1016/j.energy.2018.10.034.
[14] Kiuru T, Oijerholm M. Flexible package solutions for Siemens Sgt-800. In: 21St symp. Ind. Appl. Gas turbines comm.; 2015. October.
[15] Haglind F. Variable geometry gas turbines for improving the part-load performance of marine combined cycles - gas turbine performance. Energy 2010;35(2):562–70. https://doi.org/10.1016/j.energy.2009.10.026.
[16] Nazari B, Keshavarz MH, Roohi F. Simple method to assess autoignition temperature of organic ether compounds with high reliability for process safety. J Therm Anal Calorim 2021. https://doi.org/10.1007/s10973-021-10846-8. 0123456789.
[17] Cox JC, Hutchinson Da, Oswald JI. The westinghouse/rolls-royce WR-21 gas turbine variable area power turbine design. 1995.
[18] T. Inc., A. GT MASTER. Fayville, MA, US: Thermoflow Inc.; 2016 [Online]. Available: http://www.thermoflow.com/%0AUpdateLetters/TF8_UPDATE_LETTER.html.
[19] Manente G, Toffolo A, Lazzaretto A, Paci M. An Organic Rankine Cycle off-design model for the search of the optimal control strategy. Energy 2013;58:97–106. https://doi.org/10.1016/j.energy.2012.12.035.
[20] Saravanamuttoo HIH, Rogers GFC, Cohen H. Gas turbine theory. Pearson Education; 2001.
[21] Meitner PL, Glassman AJ. Off-design performance loss model for radial turbines with pivoting, variable-area stators. NATIONAL AERONAUTICS AND SPACE ADMINISTRATION CLEVELAND OH LEWIS RESEARCH CENTER; 1980.
[22] Hagen BAL, Agromayor R, Nekså P. Equation-oriented methods for design optimization and performance analysis of radial inflow turbines. Energy 2021;237:121596. https://doi.org/10.1016/j.energy.2021.121596.
[23] Dixon SL, Hall C. Fluid mechanics and thermodynamics of turbomachinery. Butterworth-Heinemann; 2013.
[24] Hagen BAL, Nikolaisen M, Andresen T. A novel methodology for Rankine cycle analysis with generic heat exchanger models. Appl Therm Eng 2020;165(October 2019):114566. https://doi.org/10.1016/j.applthermaleng.2019.114566.
[25] Dhar PL. Thermal system design and simulation. 2016.
[26] Ceglia F, Marrasso E, Roselli C, Sasso M. Effect of layout and working fluid on heat transfer of polymeric shell and tube heat exchangers for small size geothermal ORC via 1-D numerical analysis. Geothermics 2021;95(February):102118. https://doi.org/10.1016/j.geothermics.2021.102118.
[27] Bell IH, Wronski J, Quoilin S, Lemort V. Pure and pseudo-pure fluid thermophysical property evaluation and the open-source thermophysical property library CoolProp. Ind Eng Chem Res 2014;53(6):2498–508.